Article

Properties Optimization of Soft Magnetic Composites Based on the Amorphous Powders with Double Layer Inorganic Coating by Phosphating and Sodium Silicate Treatment

Pan Luo [1], Hongya Yu [1],*, Ce Wang [1], Han Yuan [1], Zhongwu Liu [1],*, Yu Wang [2], Lu Yang [2] and Wenjie Wu [2]

[1] School of Materials Science and Engineering, South China University of Technology, Guangzhou 510640, China
[2] Southwest Institute of Applied Magnetism, Mianyang 621000, China
* Correspondence: yuhongya@scut.edu.cn (H.Y.); zwliu@scut.edu.cn (Z.L.)

Abstract: Core-shell structured amorphous FeSiBCr@phosphate/silica powders were prepared by phosphating and sodium silicate treatment. The soft magnetic composites (SMCs) were fabricated based on these powders. The effects of phosphoric acid (H_3PO_4) concentration and annealing temperature on their properties were investigated. During the phosphating process, the powder coated with a low concentration of H_3PO_4-ethanol solution leads to uneven phosphate coating, while the peeling of phosphate coating occurs for the high H_3PO_4 concentration. Using 0.5 wt.% phosphoric solution, a uniform and dense insulation layer can be formed on the surface of the powder, resulting in increased resistivity and the reduced eddy current loss of the amorphous soft magnetic composites (ASMCs). This insulation layer can increase the roughness of the powder surface, which is beneficial to the subsequent coating of sodium silicate. By optimizing sodium silicate treatment, a complete and uniform SiO_2 layer can be formed on the phosphated powders well, leading to double layer core-shell structure and excellent soft magnetic properties. The magnetic properties of amorphous SMCs can be further improved by post annealing due to the effectively released residual stress. The enhanced permeability and greatly reduced core loss can be achieved by annealing at 773 K, but the deterioration of magnetic properties occurs as the annealing temperature over 798 K, mainly due to the increase of α-Fe(Si) and Fe_3B phases, which hinder the domain wall displacement and magnetic moment rotation. The excellent soft magnetic properties with permeability μ_e = 35 and core loss P_s = 368 kW/m^3 at 50 mT/200 kHz have been obtained when the SMCs prepared with the powders coated by 0.5 wt.% H_3PO_4 and 2 wt.% sodium silicate were annealed at 773 K.

Keywords: soft magnetic composites; amorphous powder; phosphating; sodium silicate; annealing; magnetic properties

1. Introduction

Soft magnetic composites (SMCs), consisting of soft magnetic powders and insulation binder, have found increasing applications in various electronic and electrical components due to their stable permeability and low core loss at high frequency [1–4]. With the development of magnetic devices towards miniaturization, high frequency, and high efficiency, SMCs with high magnetic saturation, stable permeability, and low core loss are urgently required [5–7]. Currently, there are various types of magnetic powders for SMCs, including pure iron (Fe), Fe-Si, Sendust (Fe-Si-Al), Flux (Fe-Ni), MPP (Fe-Ni-Mo), Fe-based amorphous, and nanocrystalline alloys. The Fe-based amorphous alloys such as FeSiBCr prepared by gas atomization exhibit high potential to work as the ideal core materials due to their good sphericity, low coercivity, and high saturation magnetization.

The preparation of SMCs involves coating an insulation layer on the metallic powders followed by powder forming and curing. Both inorganic coatings and organic coatings are employed. Inorganic coatings including oxides (SiO_2 [8–10], MgO [11], TiO_2 [12],

Al_2O_3 [13], ZrO_2 [14]), ferrites (MnZn ferrite [15], NiZn ferrite [16]) and inorganic salts exhibit high temperature resistance and high electric resistivity. They are generally prepared by in-situ chemical synthesis or coating a mixture of inorganic nanoparticles and organic resin on the powder. However, it was found that, for the oxide coating, a uniform and dense layer tightly bound to the magnetic powder is difficult to prepare. Soft magnetic ferrites can be used for coating, which exhibits high resistivity and high magnetization, but the brittle ferrite layer is easy to break during the pressing process. The inorganic salt layer can be prepared by direct reaction of the acid with the magnetic powder [15]. These coatings have the advantages of high density, high uniformity, high resistivity, and strong bonding with the magnetic powder. The common acids include HNO_3 [17,18] and H_3PO_4 [19,20], among which H_3PO_4 is frequently used for industrial production. However, for the amorphous Fe-based alloy powders, it is difficult to prepare an insulating layer on their surfaces by H_3PO_4 treatment [21] since amorphous alloys generally show excellent corrosion resistance [22].

It has been reported [8] that silica (SiO_2) coating can work as effective high-resistive thin layer for the magnetic powders. Sol-gel method is generally employed for preparing SiO_2 coating on Fe-based powder, but this process is complicated since four kinds of chemicals including tetraethoxysilane (TEOS) are needed [23]. Recently, FeSiCr powder was coated with a SiO_2 layer by reacting carbon dioxide with sodium silicate, which indicates that sodium silicate (Na_2SiO_3) can be used as a silicon source [24]. However, the insulating layer prepared by sodium silicate is not dense (in particular for the atomized amorphous powder with the smooth surface).

In this work, in order to obtain a uniform and dense insulation layer on the amorphous Fe-based alloy powder, an inorganic double layer coating is proposed, which was prepared by phosphating followed by SiO_2 coating. The phosphating layer by H_3PO_4 treatment is employed to increase the surface roughness of the powder, which is beneficial for depositing a uniform and dense insulation SiO_2 layer. By this approach, we prepared core-shell structured amorphous FeSiBCr@phosphate/SiO_2 powders, which then were made into magnetic cores. The effects of H_3PO_4 concentration and annealing temperature on the soft magnetic properties of SMCs were investigated. This method is suitable for the industrial production of amorphous SMCs with stable permeability and low core loss.

2. Experimental Procedures

Commercial gas atomized $Fe_{87}Si_{5.5}B_4Cr_{3.5}$ amorphous powders were supplied by Tiz-Advanced Alloy Technology Co., Ltd (Quanzhou, China). The average particle size D50 of the raw powders is approximately 20 μm and the *apparent density of powders* is 3.5–4.0 g/cm^3. The saturation magnetization (M_s) of the raw powders is 148 Am^2/kg. Sodium silicate (Na_2SiO_3) with modulus of 1 is purchased from Guangzhou Chemical Reagent Factory (Guangzhou, China). To prepare SMCs, the FeSiBCr powders (30 g) were first dispersed in H_3PO_4-ethanol solution (30 g) with various H_3PO_4 concentrations (0 wt.%, 0.25 wt.%, 0. 5 wt.%, 0.75 wt.%, 1.0 wt.%) under constant stirring at 55 °C until the ethanol solvent was completely evaporated for surface passivation. After washing and drying, the phosphated powders were obtained. The phosphatized powders were then dispersed in 2 wt.% sodium silicate aqueous solution (15 g) and stirred at 328 K for 20 min. The obtained magnetic powders were filtered and washed with deionized water for three times. The treated powders were mixed with 2.5 wt.% silicone resin and 0.5 wt.% epoxy resin-acetone solution and stirred at room temperature until the acetone solvent evaporated completely for binding. The bonded powders were compacted into toroidal-shaped amorphous SMCs with the dimensions of $\Phi20 \times \Phi12 \times 4$ mm under 1200 MPa for 5.5 s. The SMCs were cured at 453 K for 1 h. For annealing treatment, the selected amorphous SMCs were heated at different temperatures (748, 773, 798 K) for 1 h under Ar atmosphere.

The surface morphologies of the powders were observed by scanning electron microscopy (SEM, FEI Quanta 200, Hillsboro, OR, USA). Fourier transform infrared spectrometer (FTIR, VERTEX 70, Bruker, Billerica, MA, USA) was used to investigate the

phase constitution of the insulation layer. The soft magnetic properties were obtained by LCR meter (IM3536, Hioki, Nagano, Japan) and soft magnetic AC measurement device (MATS-3010SA, Linkjoin, Loudi, China). The electrical resistivity was measured by a high resistance weak current tester (ST2643, Jingge, SuZhou, China). The phase structures of powders were confirmed by X-ray diffraction (XRD, Philips X' Pert, PANalytical, Almelo, The Netherlands) using Cu Kα radiation at room temperature in the range of 20–80°. The magnetic hysteresis loops were measured at room temperature using a vibrating sample magnetometer (VSM, East Changing, Beijing, China). The radial crush strength was measured by core rupture test machine (FL-8621, Feiling, Dongguan, China).

3. Results and Discussion

3.1. The Formation of Double Layer Structure on the Powder

Figure 1 shows the SEM images of the amorphous FeSiBCr powders before and after different treatments. In Figure 1a, the original powder shows smooth surface, which is unfavorable for the coating of sodium silicate through physical contact. The surface of the powder after phosphatized in a 0.5 wt.% H_3PO_4-ethanol solution becomes rough, as shown in Figure 1b. The rough phosphate structure can improve the adhesion of sodium silicate. After treated only by sodium silicate, the powder surface exhibits loose and porous structure (Figure 1c). A dense insulating layer can be formed on the surface of the powder after two-step treatment by both H_3PO_4 and sodium silicate, as shown in Figure 1d. As we know, the uniform and dense insulation layer on the powders is beneficial to the soft magnetic properties of SMCs.
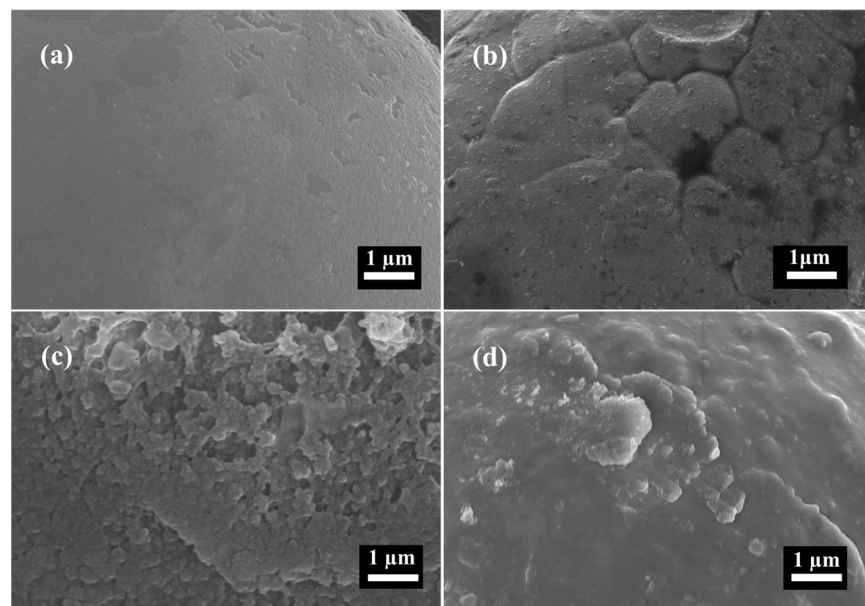

Figure 1. SEM images of (**a**) the original powder and the powders treated by (**b**) 0.5 wt.% H_3PO_4-ethanol solution, (**c**) 2 wt.% sodium silicate-aqueous solution, and (**d**) 0.5 wt.% H_3PO_4-ethanol solution followed by 2 wt.% sodium silicate-aqueous solution.

FTIR analysis results for the amorphous FeSiBCr powder and the powders after different treatments are shown in Figure 2. FTIR Curve (a) for the original powders shows no distinct band. Bands of 2915 cm^{-1} (Curve (b) and (c)) are attributed to the-CH$_3$ group from residual C_2H_5OH. The characteristic peaks of phosphate are observed at the band of 1065 cm^{-1} and 540 cm^{-1} for the powders treated by H_3PO_4-ethanol solution (Curve (b)). The bands at 1640 cm^{-1} and 1065 cm^{-1} are assigned to the bending mode of P-OH bonds and the symmetric stretching vibrations of P-O bonds [25], respectively. The results indicate that the phosphate has been formed on the surface of the magnetic powder after H_3PO_4 treatment. On Curve (c) for the powders coated by sodium silicate-aqueous solution, the

broad absorption band at 1038 cm^{-1} originates from the symmetric vibration absorption of Si-O-Si [26], which confirms that the obtained coating layer on the powders is SiO$_2$. On Curve (d) for the powders treated with H$_3$PO$_4$-ethanol followed by sodium silicate solution, the characteristic bonds of both phosphate and SiO$_2$ can be detected, indicating that both phosphate and SiO$_2$ layers are formed on the powders. Compared with phosphate and SiO$_2$ coating alone, the hybrid phosphate-SiO$_2$ layer exhibits significantly decreased intensity of the absorption peak corresponding to -OH at 3450 cm^{-1}, indicating that the -OH of phosphate binds to the -OH of sodium silicate. The results thus suggest that the P-O-Si bond may be formed on the powder, which can enhance the binding of SiO$_2$ and magnetic powder.
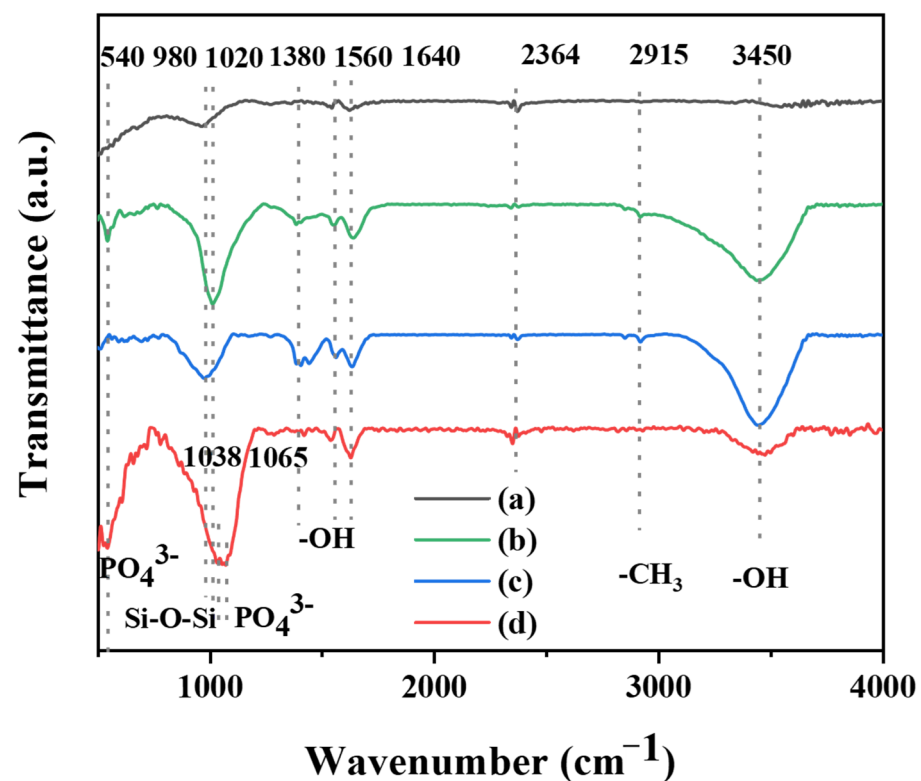

Figure 2. FTIR curves of (**a**) the original FeSiBCr powders, and the powders treated by (**b**) H$_3$PO$_4$-ethanol solution, (**c**) sodium silicate-aqueous solution, and (**d**) H$_3$PO$_4$-ethanol solution followed by sodium silicate-aqueous solution.

The evolution of the core-shell structure on the magnetic powder can be illustrated in Figure 3. In the first step 1, H$_3$PO$_4$ reacts with the FeSiBCr powder according to Equation (1), and the first layer of phosphate can be formed on the powder [27,28]. In the second step, Si(OH)$_4$ dehydrates and condenses with the -OH on the phosphated powder surface to form a networked SiO$_2$, and the second shell on the powder is formed. Hydrolysis reaction and condensation reaction can be expressed by Equations (2) and (3) [29]. As a result, the core-shell structured FeSiBCr@phosphate/SiO$_2$ powders can be prepared.
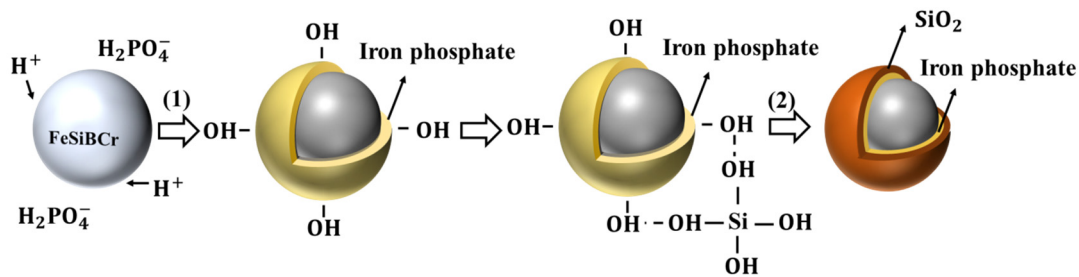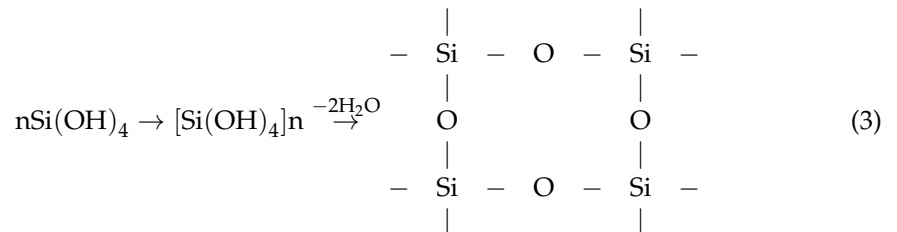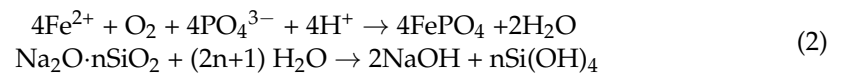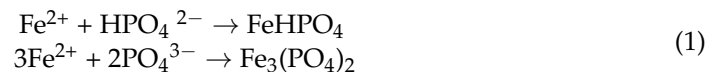
Figure 3. Evolution of the core-shell structure of magnetic powder. (**1**) Phosphate coating process; (**2**) SiO_2 coating process.

$$Fe^{2+} + HPO_4{}^{2-} \rightarrow FeHPO_4$$
$$3Fe^{2+} + 2PO_4{}^{3-} \rightarrow Fe_3(PO_4)_2 \tag{1}$$

$$4Fe^{2+} + O_2 + 4PO_4{}^{3-} + 4H^+ \rightarrow 4FePO_4 + 2H_2O$$
$$Na_2O \cdot nSiO_2 + (2n+1)\,H_2O \rightarrow 2NaOH + nSi(OH)_4 \tag{2}$$

$$nSi(OH)_4 \rightarrow [Si(OH)_4]n \xrightarrow{-2H_2O} \quad
\begin{array}{ccccc}
| & & & & | \\
-\;Si & - & O & - & Si\; - \\
| & & & & | \\
O & & & & O \\
| & & & & | \\
-\;Si & - & O & - & Si\; - \\
| & & & & |
\end{array} \tag{3}$$

3.2. Effects of Phosphated by Various H_3PO_4 Concentrations

Figure 4a–d show the SEM images of the powders phosphated by the H_3PO_4 with different concentrations (0.25 wt.%, 0.5 wt.%, 0.75 wt.%, 1.0 wt.%). For the powder phosphated with 0.25 wt.% H_3PO_4, P and O elements are evenly distributed on the powder surface, as shown in Figure 4a with EDS result. It is believed that a phosphating layer is formed. Comparing the morphologies in Figure 4a–d, the higher concentration of H_3PO_4 leads to the rougher surface of the powder. When the H_3PO_4 concentration increases to 1 wt.%, a large amount of sheet structures appears. EDS testing shows that these sheet structures contain abundant P, O, and Fe elements, presumably phosphate, as shown in Figure 4d. The appearance of the sheet structured phosphate may destroy the integrity of the layer and reduce the density of the SMCs. Thus, it is necessary to control the nucleation and precipitation of the flaky phosphate to make the phosphate coating strong and dense.

Table 1 shows the effective permeability μ_e, quality factor Q and core loss P_s of the magnetic cores prepared from the powders treated with 0.5 wt.% H_3PO_4-ethanol solution followed by different concentrations of sodium silicate solution. All cores were annealed at 773 K for 1 h. It was found that an appropriate amount of SiO_2 can help to form a uniform and complete insulation layer on the powders, which will not completely break during the pressing process. However, more SiO_2 with high hardness may result in decreased density and deteriorated magnetic properties [30]. The core based on powders experienced 2 wt.% sodium silicate solution offer the optimal performance with high permeability, high Q, and low magnetic loss. Therefore, in the following experiments, for studying the effects of H_3PO_4 concentration on the properties of SMCs, 2 wt.% sodium silicate-aqueous solution were selected for coating SiO_2.
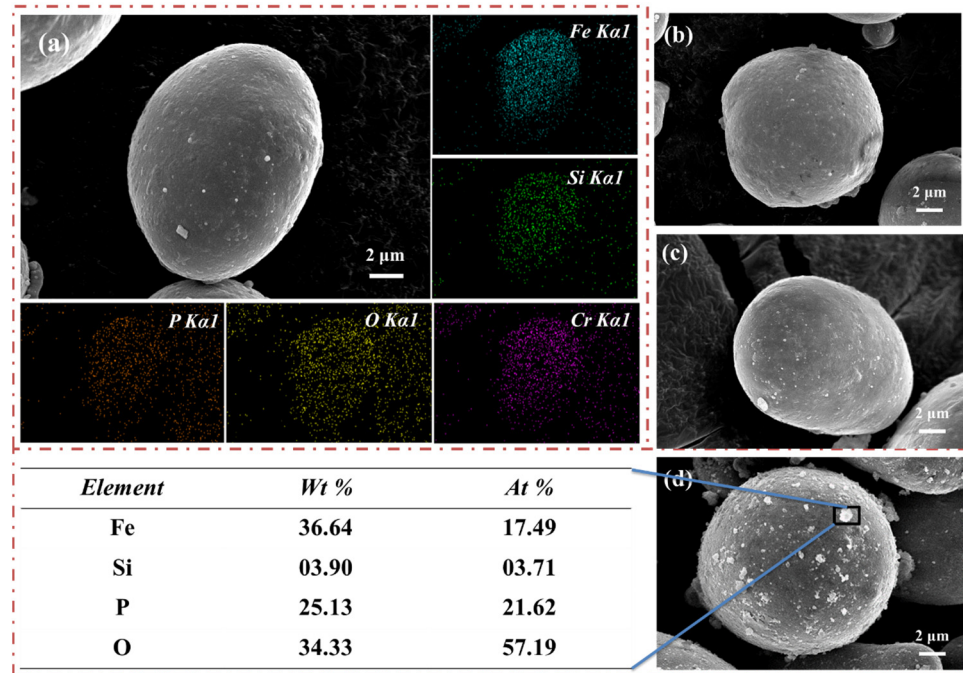
Figure 4. SEM images of the powders phosphated by different H_3PO_4 concentrations (**a**) 0.25 wt.%, (**b**) 0.5 wt.%, (**c**) 0.75 wt.%, and (**d**) 1.0 wt.%. The EDS result of powder phosphated by H_3PO_4 concentration of 0.25 wt.% is also shown in the figure.

Table 1. Effective permeability μ_e, Q and core loss P_s of the SMCs with 0.5 wt.% H_3PO_4-ethanol solution and different concentration of sodium silicate-aqueous solution.

Sample (Powder Treatment)	Effective Permeability (μ_e)	Q	Ps (kW/m^3)	
			50 mT/100 kHz	50 mT/200 kHz
Phosphatized 0.5 wt.%	37.8	42	301.0	703.6
Phosphatized 0.5 wt.% + Sodium silicate 1 wt.%	36.4	35	243.6	576.3
Phosphatized 0.5 wt.% + Sodium silicate 2 wt.%	33.4	50	136.4	368.0
Phosphatized 0.5 wt.% + Sodium silicate 3 wt.%	32.0	45	187.1	490.3
Phosphatized 0.5 wt.% + Sodium silicate 4 wt.%	29.0	35	194.3	564.6

Figure 5 shows the magnetic properties of SMCs fabricated by the amorphous FeSiBCr powders treated with various H_3PO_4-ethanol solutions followed by 2 wt.% sodium silicate-aqueous solution and annealed at 773 K. For all samples, the permeability decreases as the frequency increases, mainly due to the weakening effect of eddy currents generated by induced electromotive force on the applied magnetic field at high frequencies (Figure 5a). It decreases from ~37.8 to ~29.0 with increasing H_3PO_4 concentration from 0 to 1 wt.%. Increasing H_3PO_4 concentration leads to more non-magnetic material, resulting in lower permeability. When the H_3PO_4 concentration is 0.5 wt.%, the SMCs has the beat frequency stability, as shown in Figure 2. The insulating layer prepared by 0.5 wt.% H_3PO_4 concentration followed by 2 wt.%Na_2SiO_3 has the beat coating effect and can effectively isolate eddy currents between powders.
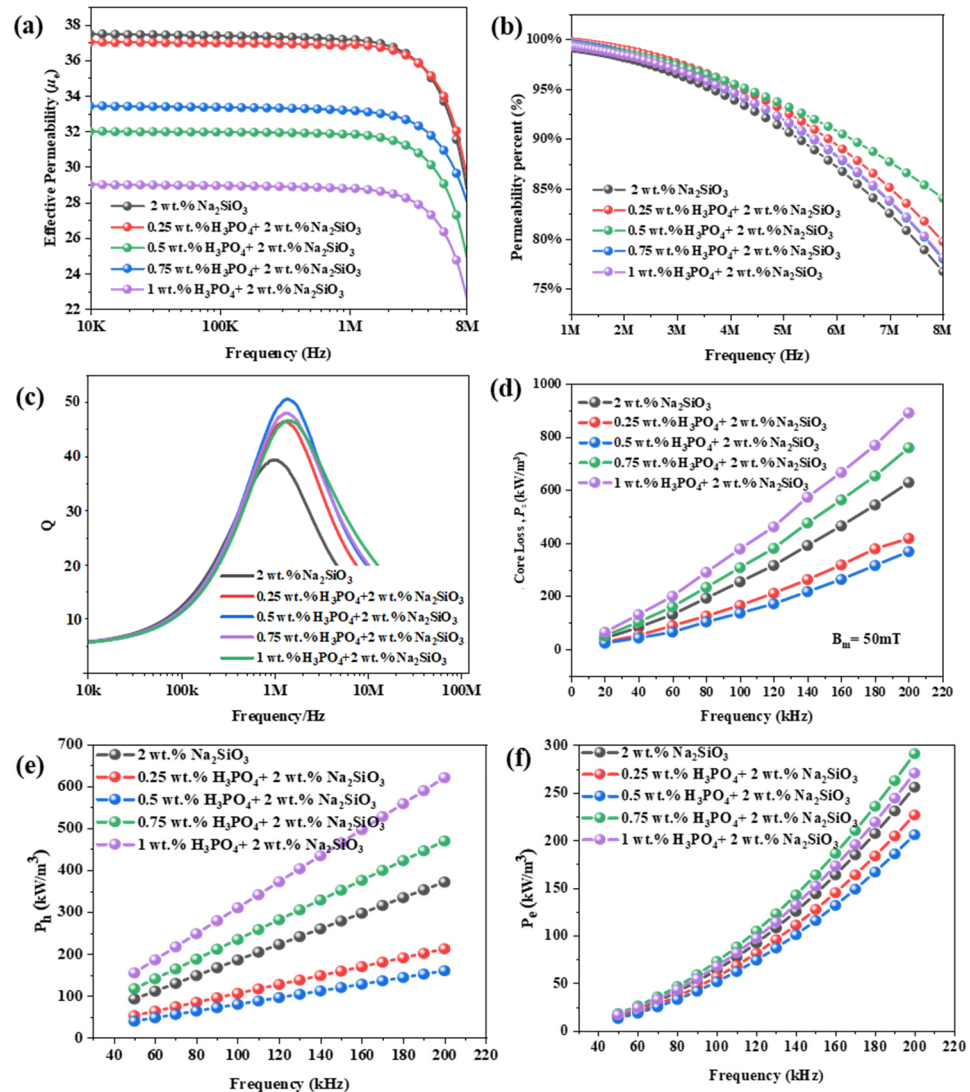
Figure 5. Frequency dependences of the (**a**) μ_e, (**b**) permeability percent, (**c**) Q, (**d**) P_s, (**e**) P_h, (**f**) P_e for SMCs after coating with different H_3PO_4 concentrations.

Q value is the quality factor, which is an important indicator to measure the high-frequency performance of soft magnetic composites. The Q value can be expressed by the ratio of the real permeability μ of the soft magnetic composite to the imaginary permeability μ', as well as the ratio of the inductance and the equivalent loss resistance, expressed as Equation (4):

$$Q = \frac{\mu'}{\mu''} = \left(\frac{2\pi f L_s}{R_s}\right) \tag{4}$$

where L_s is the inductance and R_s is the equivalent loss resistance. In general, the higher the Q value on behalf of powder cores, the lower the rate of energy loss. The Q value of the sample first increases then decreases with increasing frequency (Figure 5b). The SMCs treated with 0.5 wt.% H_3PO_4 concentration exhibits a maximum peak value of 50, which shows a significant performance improvement compared to those without H_3PO_4 treatment.

The frequency dependence of core loss (P_s) for the SMCs prepared with different H_3PO_4 concentrations in the range of 20 kHz to 200 kHz at B_m = 50 mT are shown in Figure 5c. The P_s of all samples increase rapidly with increasing frequency. The lowest P_s of 368 kW/m^3 at 200 kHz is obtained for the SMC with 0.5 wt.% H_3PO_4 concentration, decreased by 41% compared to that without phosphating. P_s decreases from 628 to

368 kW/m^3 until the H$_3$PO$_4$ concentration increases from 0 to 0.5 wt.%. As the concentration of H$_3$PO$_4$ exceeds 0.5 wt.%, the P_s shows a rapid increase. As we know, P_s is mainly determined by the hysteresis loss (P_h), the eddy loss (P_e) and residual loss (P_r), which can be expressed by Equation (5) [31]:

$$P_{s\text{ (total)}} = P_h + P_e + P_r \approx f \oint H dB + \frac{CB^2 d^2 f^2}{\rho} + \mathrm{K_r Bxf^{1.5}} \tag{5}$$

$$P_e = P_e^{\text{Intra}} + P_e^{\text{Inter}} = \frac{(\pi d_{\text{powder}} B_m)^2}{20\rho_{\text{powder}} R_{\text{powder}}} f^2 + \frac{(\pi d_{\text{eff}} B_m)^2}{\beta \rho_s R_s} f^2 \tag{6}$$

where H is the magnetic field, B is the magnetic flux density, f is the frequency, C is the constant, d is the effective diameter of powders and ρ is the resistivity. K_r is residual loss coefficient related to the material, and x is the coefficient related to the magnitude and frequency of the applied magnetic field. P_r is a combination of relaxation and resonant losses. These losses are only important at very low induction levels and very high frequencies and can be ignored in power applications [1,32,33]. Eddy current losses include intra-particle and inter-particle eddy current losses, as shown in Equation (6), d_{powder} is the effective size of the powder, ρ_{powder} is the density of the powder, and R_{powder} is the resistivity of the powder. d_{eff} is the effective size of the eddy current, ρ_s is the density of the SMCs, and R_s is the resistivity of the SMCs. P_e^{Intra} is mainly related to the resistivity and particle size of the powder. P_e^{Inter} is mainly related to the degree of insulation between powder particles, that is, the resistivity of SMCs. In this paper, by using different insulation coating processes, the Rs of the SMCs can be effectively improved, thereby reducing the P_e^{Inter}.

P_s can be separated into P_h and P_e based on above equation and the results are presented in Figures 5d and 5e, respectively. When the H$_3$PO$_4$ concentration exceeds 0.5 wt.%, P_h and P_e increase with the increase of H$_3$PO$_4$ concentration. This can be understood since the excess iron phosphate precipitates between the soft magnetic composite particles [34]. Sodium silicate can react with dehydration and condensation on the detached phosphate layer, which worsens the coating effect of the magnetic powder, leading to the increase of P_h and P_e. The reduced P_e is mainly due to the electrical resistivity reduction resulting from the destruction of the layer, as shown in Figure 6.
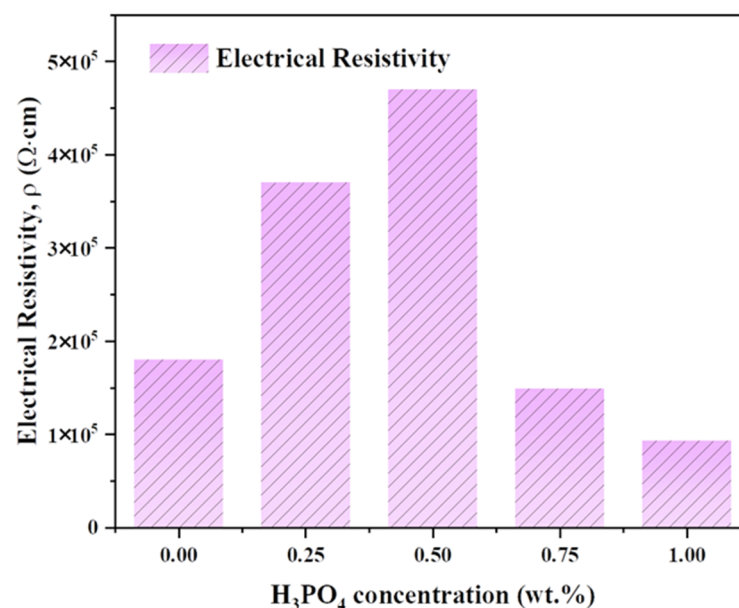

Figure 6. Electrical resistivity for SMCs after coating with different H$_3$PO$_4$ concentrations.

The magnetic composite consists of core and surface layer. For a spherical magnetic particle coated with a layer, the saturation magnetization (M_S) can be expressed as Equation (7),

$$M_S = \frac{M_{SP} \cdot V_P + M_{SL} \cdot V_L}{V_P + V_L} = M_{SP} - \frac{6t}{d}(M_{SP} - M_{SL}) \tag{7}$$

where d and t represent the diameter of magnetic particle and the thickness of surface layer, respectively. M_{SP} and M_{SL} are the saturation magnetizations of the particle and layer, respectively. V corresponds to the volume [35]. The hysteresis loops of FeSiBCr powders treated by different processes are recorded in Figure 7. The powders show a typical characteristic of soft magnetic material, including a high saturated magnetization and a low coercivity. The maximum M_s of raw FeSiBCr powders is 148 Am^2/kg. After treated by H_3PO_4 (0.5 wt.%) and sodium silicate (2 wt.%), the M_s decreases to 145 Am^2/kg and to 137 Am^2/kg, respectively. However, when coated with phosphate followed by SiO_2, M_s is 143 Am^2/kg, and this value is somewhere between the phosphate and SiO_2 coating alone. Compared with the layer of SiO_2, the layer of hybrid phosphate and SiO_2 has a lower M_{SL} due to the increase of non-magnetic substances. The increased M_S value for the powders coated with phosphate and SiO_2 indicated that the thickness t of the phosphate-SiO_2 layer is less than that of SiO_2 layer according to Equation (5). The results show that the double layer coating has a higher density, which gives a smaller thickness. As a result, the SMC prepared with core-shell structured FeSiBCr@phosphate/SiO_2 powders exhibits the best soft magnetic properties.
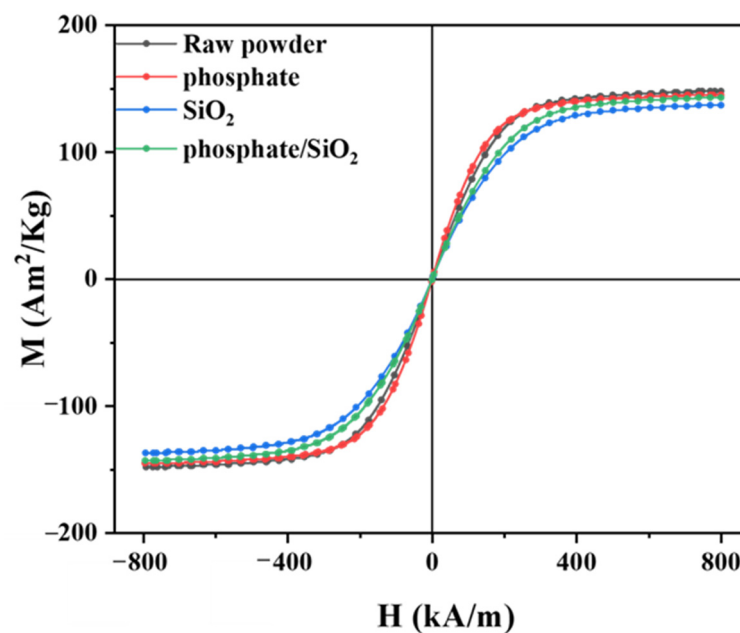

Figure 7. Magnetic hysteresis curves of FeSiBCr powders for different treatment processes.

3.3. Effects of Annealing Treatment

Figure 8a shows the variation of the effective permeability (μ_e) with frequency for SMCs treated by H_3PO_4 (0.5 wt.%) and sodium silicate (2 wt.%) followed by annealing at different temperatures. With the increasing annealing temperature from 748 to 773 K, the μ_e increases from 28.1 to 33.4. In general, the increased annealing temperature can decrease the internal stress of magnetic powder core, thereby reducing the difficulty of magnetic domain reversal and increasing the permeability [36]. The internal stress for SMCs after annealing at 748 K is released incompletely. With further elevating the annealing temperature to 773 K, the internal stress within the particles was almost removed, leading to the increase of μ_e. When the annealing temperature increases to 798 K, the μ_e of the SMCs decreases sharply to 28.0. For the SMCs annealed at 773 K, the μ_e reaches the highest

value of 33.4, increased by 43%, compared with the μ_e of 18.9 for that without annealing treatment. Similarly, due to the stress release, the quality factor (Q) shows a peak value of 50 at a frequency of 3 MHz after annealing at 773 K (Figure 8b). The minimum core loss is also obtained for the SMC annealed at 773 K (Figure 8c).
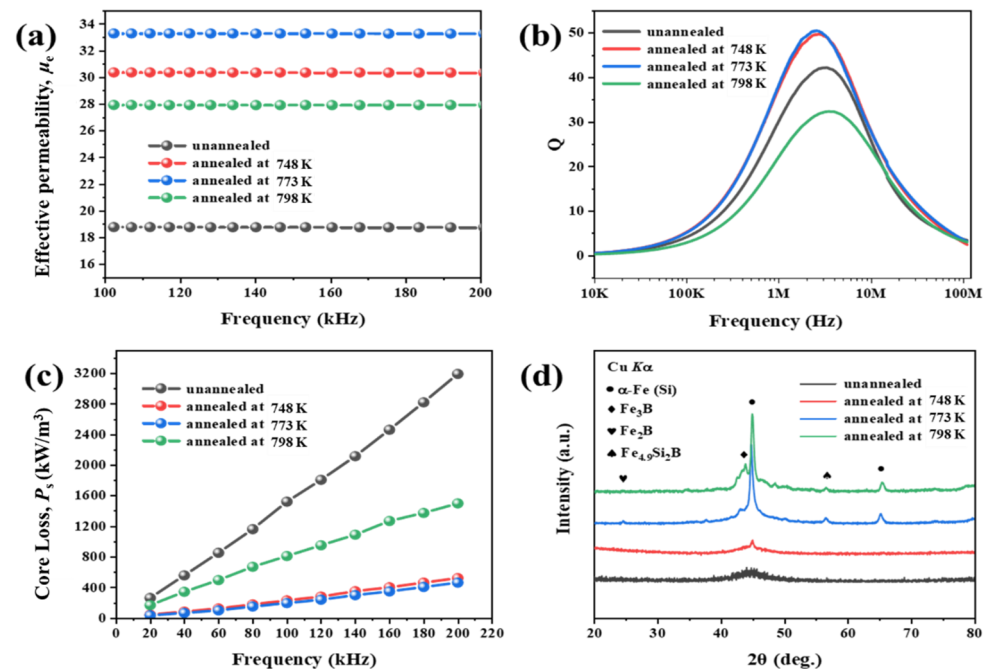

Figure 8. Frequency dependence of the (**a**) μ_e, (**b**) Q, (**c**) P_s, (**d**) XRD for SMCs after annealing at different temperatures.

To illustrate the reasons for the deterioration of magnetic properties after annealing above 798 K, the magnetic powders were tested for XRD, as shown in Figure 7. For the original powders without annealing, only one broad diffraction peak can be observed, indicating a typical amorphous structure [37]. For the powders annealed at the temperatures below 748 K, a slightly intense α-Fe (Si) phase begins to appear. The crystallization occurred after the sample annealed at 773 K, with the precipitation of α-Fe(Si) and Fe_3B phases. When the annealed temperature rises to 798 K, the intensity of Fe_3B phase increases. Compared with the soft magnetic phase of α-Fe(Si). the Fe_3B phase has a higher anisotropic field, resulting in decreased soft magnetic properties of the SMCs [38]. The average grain size D of α-Fe(Si) annealed at 773 K is approximately 18 nm calculated by the Scherrer formula. These nano-sized grains are randomly dispersed in the residual amorphous matrix. When D < L_{ex} (L_{ex} is value of ferromagnetic exchange length, about 30~40 nm for α-Fe), with the reduction of grain size, the effective anisotropy shows a sharp decrease and the impact is negligible. The magnetic domain structure exhibits a vortex structure determined by the exchange coupling energy and demagnetization energy jointly, the coercive force and residual magnetism are close to zero. Therefore, the magnetic powders after annealing at 773 K have excellent soft magnetic properties [39,40].

3.4. DC-Bias Properties

The presence of DC current or voltage components in an AC power system is called DC bias. The DC-bias property is important for SMC since almost all of the powder cores are used in a DC-bias field. Figure 9 shows the percentage of permeability as a function of the DC-bias field for SMC cores, which were made from the powders coated with different H_3PO_4 concentrations followed by 2 wt.% sodium silicate solution and annealed at 773 K. The permeability decreases with the increase of the bias field for all cores, since the SMCs approach to magnetic saturation at high DC field. In addition, with the increase

of H_3PO_4 concentrations from 0 to 0.75 wt.%, the DC-bias performance of the core, defined by the percentage of reduced permeability, increased from 75.3 to 88.2% at 4000 A/m. The results indicate that the H_3PO_4 and sodium silicate double-layer coating can significantly improve the DC bias performance of SMCs. In particular, the SMCs prepared with H_3PO_4 concentrations of 0.5 and 0.75 wt.% exhibit relatively superior DC-bias performances (over 80%). The reason is that the voids and gaps in the powder cores can pin the domain wall in the magnetizing process and prevent the propagation of domain movement between particles, then suppressing the decrease of permeability, which is beneficial in achieving a stable percent permeability [41].
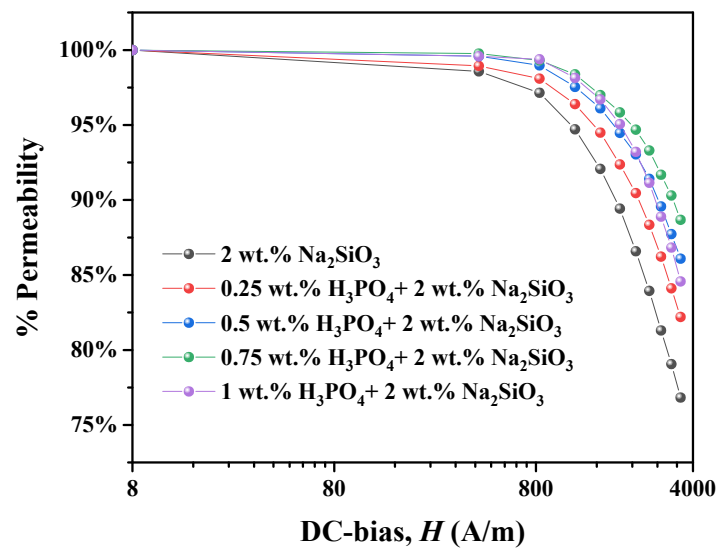

Figure 9. The variation of the permeability with the DC-bias field for SMCs after coating with different H_3PO_4 concentrations.

3.5. Radial Crushing Properties

The SMCs based on powders coated by different H_3PO_4 concentrations and 2 wt.% sodium silicate-aqueous solution followed by annealed at 773 K is employed for radial crush testing. The test method is shown in Figure 10a, where the radial crush strength of a ring shape specimen is determined by applying radial pressure. Figure 10b shows the radial crush strength of various SMCs. The strength first increases then decreases with the increasing concentration. The $Si(OH)_4$ produced by hydrolysis of sodium silicate, through dehydration and condensation between -OH can form networked SiO_2 between the magnetic powders, which can increase the binding force between the magnetic powders. When the powders coated by 2 wt.% sodium silicate-aqueous solution alone, the binding force between the powder is poor due to the weak binding force between SiO_2 and powders, which is manifested by the low radial crush strength of the SMCs. As the H_3PO_4 concentration increases, the radial crush strength increases since the rough surface of the phosphate can increase the binding force with SiO_2, while the binding force between the powders also increases. However, when the H_3PO_4 concentration exceeds 0.5 wt.%, the radial crush strength of the sample decreases, since part of the SiO_2 forms on sheets detached from phosphate layer.
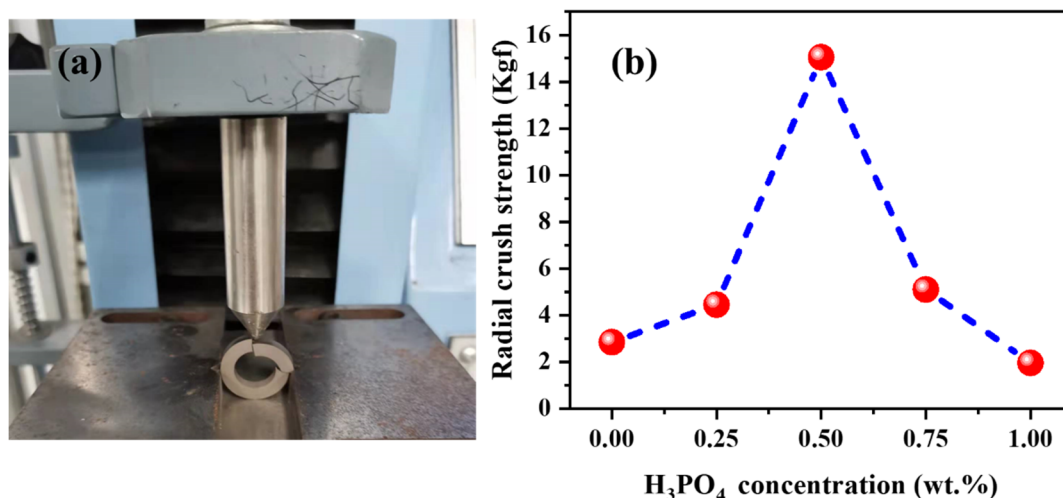
Figure 10. (**a**)The radial crush test method and (**b**) the radial crush strength of SMCs based on powders prepared by different H_3PO_4 concentration followed by 2 wt.% sodium silicate-aqueous solution after annealing.

4. Conclusions

The core-shell structured amorphous FeSiBCr@phosphate/SiO_2 powders were prepared by H_3PO_4 and sodium silicate treatments for fabricating high performance SMCs. The processes of phosphating, sodium silicate coating and annealing treatment have been investigated in detail. A complete and uniform phosphate/SiO_2 doubled layer has been prepared on the amorphous powder by 0.5 wt.% H_3PO_4 followed by 2 wt.% sodium silicate treatments. When the H_3PO_4 concentration exceeds to 0.5 wt.%, the phosphate sheets were detached from phosphate layer, leading to poor powder coating efficiency and poor performance of SMC. After annealing at 773 K, the SMCs show improved permeability and greatly reduced core loss due to the effectively released residual stress. However, when the annealing temperature is 798 K, the soft magnetic properties including permeability and core loss were deteriorated due to the increasing precipitation of Fe_3B phase. The excellent magnetic properties with permeability $\mu_e = 33.5$ and core loss $P_s = 368$ kW/m^3 at 50 mT and 200 kHz have been achieved in the SMC prepared by optimized process. i.e., 0.5 wt.% H_3PO_4 -ethanol solution and 2 wt.% sodium silicate-aqueous solution treatment followed by 773 K annealing, which promises great potential applications of electronic components at medium and high frequencies.

Author Contributions: Conceptualization, P.L. and C.W.; methodology, P.L. and H.Y. (Han Yuan); software, P.L.; validation, P.L., H.Y. (Hongya Yu) and Z.L.; formal analysis, P.L.; investigation, P.L. and C.W.; resources, H.Y. (Han Yuan); data curation, P.L.; writing—original draft preparation, P.L.; writing—review and editing, H.Y. (Hongya Yu), Z.L., and P.L.; visualization, C.W.; supervision, Z.L., Y.W., L.Y. and W.W.; project administration, H.Y. (Hongya Yu), Z.L.; funding acquisition, Y.W., L.Y. and W.W.; All authors have read and agreed to the published version of the manuscript.

Data Availability Statement: Not applicable.

Conflicts of Interest: The authors declare no conflict of interest.

References

1. Shokrollahi, H.; Janghorban, K. Soft magnetic composite materials (SMCs). *J. Mater. Process. Technol.* **2007**, *189*, 1–12. [CrossRef]
2. Sunday, K.J.; Taheri, M.L. Soft magnetic composites: Recent advancements in the technology. *Met. Powder Rep.* **2017**, *72*, 425–429. [CrossRef]

3. Périgo, E.A.; Weidenfeller, B.; Kollár, P.; Füzer, J. Past, present, and future of soft magnetic composites. *Appl. Phys. Rev.* **2018**, *5*, 031301. [CrossRef]

4. Silveyra, J.M.; Ferrara, E.; Huber, D.L.; Monson, T.C. Soft magnetic materials for a sustainable and electrified world. *Science* **2018**, *362*, 418–427. [CrossRef]

5. Makino, A.; Kubota, T.; Makabe, M.; Chang, C.T.; Inoue, A. FeSiBP metallic glasses with high glass-forming ability and excellent magnetic properties. *Mater. Sci. Eng. B* **2008**, *148*, 166–170. [CrossRef]

6. Wang, J.; Li, R.; Hua, N.; Huang, L.; Zhang, T. Ternary Fe–P–C bulk metallic glass with good soft-magnetic and mechanical properties. *Scr. Mater.* **2011**, *65*, 536–539. [CrossRef]

7. Li, Z.; Wang, A.; Chang, C.; Wang, Y.; Dong, B.; Zhou, S. Synthesis of FeSiBPNbCu nanocrystalline soft-magnetic alloys with high saturation magnetization. *J. Alloys Compd.* **2014**, *611*, 197–201. [CrossRef]

8. Sun, H.; Wang, C.; Wang, J.; Yu, M.; Guo, Z. Fe-based amorphous powder cores with low core loss and high permeability fabricated using the core-shell structured magnetic flaky powders. *J. Magn. Magn. Mater.* **2020**, *502*, 166548. [CrossRef]

9. Wang, C.; Guo, Z.; Wang, J.; Sun, H.; Chen, D.; Chen, W.; Liu, X. Industry-oriented Fe-based amorphous soft magnetic composites with SiO2-coated layer by one-pot high-efficient synthesis method. *J. Magn. Magn. Mater.* **2020**, *509*, 166924. [CrossRef]

10. Zhou, B.; Dong, Y.; Chi, Q.; Zhang, Y.; Chang, L.; Gong, M.; Huang, J.; Pan, Y.; Wang, X. Fe-based amorphous soft magnetic composites with SiO_2 insulation coatings: A study on coatings thickness, microstructure and magnetic properties. *Ceram. Int.* **2020**, *46*, 13449–13459. [CrossRef]

11. Zhang, Y.; Zhou, T.d. Structure and electromagnetic properties of FeSiAl particles coated by MgO. *J. Magn. Magn. Mater.* **2017**, *426*, 680–684. [CrossRef]

12. Zhou, B.; Dong, Y.; Liu, L.; Chi, Q.; Zhang, Y.; Chang, L.; Bi, F.; Wang, X. The core-shell structured Fe-based amorphous magnetic powder cores with excellent magnetic properties. *Adv. Powder Technol.* **2019**, *30*, 1504–1512. [CrossRef]

13. Peng, Y.; Yi, Y.; Li, L.; Yi, J.; Nie, J.; Bao, C. Iron-based soft magnetic composites with Al_2O_3 insulation coating produced using sol–gel method. *Mater. Des.* **2016**, *109*, 390–395. [CrossRef]

14. Geng, K.; Xie, Y.; Yan, L.; Yan, B. Fe-Si/ZrO_2 composites with core-shell structure and excellent magnetic properties prepared by mechanical milling and spark plasma sintering. *J. Alloys Compd.* **2017**, *718*, 53–62. [CrossRef]

15. Wang, Z.; Liu, X.; Kan, X.; Zhu, R.; Yang, W.; Wu, Q.; Zhou, S. Preparation and characterization of flaky FeSiAl composite magnetic powder core coated with MnZn ferrite. *Curr. Appl. Phys.* **2019**, *19*, 924–927. [CrossRef]

16. Birčáková, Z.; Onderko, F.; Dobák, S.; Kollár, P.; Füzer, J.; Bureš, R.; Fáberová, M.; Weidenfeller, B.; Bednarčík, J.; Jakubčin, M.; et al. Eco-friendly soft magnetic composites of iron coated by sintered ferrite via mechanofusion. *J. Magn. Magn. Mater.* **2022**, *543*, 168627. [CrossRef]

17. Liu, D.; Wu, C.; Yan, M.; Wang, J. Correlating the microstructure, growth mechanism and magnetic properties of FeSiAl soft magnetic composites fabricated via HNO_3 oxidation. *Acta Mater.* **2018**, *146*, 294–303. [CrossRef]

18. Wei, H.; Yu, H.; Feng, Y.; Wang, Y.; He, J.; Liu, Z. High permeability and low core loss nanocrystalline soft magnetic composites based on FeSiBNbCu@Fe_3O_4 powders prepared by HNO_3 oxidation. *Mater. Chem. Phys.* **2021**, *263*, 124427. [CrossRef]

19. Yu, H.; Zhou, S.; Zhang, G.; Dong, B.; Meng, L.; Li, Z.; Dong, Y.; Cao, X. The phosphating effect on the properties of FeSiCr alloy powder. *J. Magn. Magn. Mater.* **2022**, *552*, 168741. [CrossRef]

20. Chen, Z.; Liu, X.; Kan, X.; Wang, Z.; Zhu, R.; Yang, W.; Wu, Q.; Shezad, M. Phosphate coatings evolution study and effects of ultrasonic on soft magnetic properties of FeSiAl by aqueous phosphoric acid solution passivation. *J. Alloys Compd.* **2019**, *783*, 434–440. [CrossRef]

21. Ding, W.; Jiang, L.; Li, B.; Chen, G.; Tian, S.; Wu, G. Microstructure and Magnetic Properties of Soft Magnetic Composites with Silicate Glass Insulation Layers. *J. Supercond. Novel. Magn.* **2013**, *27*, 239–245. [CrossRef]

22. Wang, D.L.; Ding, H.P.; Ma, Y.F.; Gong, P.; Wang, X.Y. Research progress on corrosion resistance of metallic glasses. *J. Chin. Soc. Corros. Prot.* **2021**, *41*, 277–288.

23. Chen, S.F.; Chang, H.Y.; Wang, S.J.; Chen, S.H.; Chen, C.C. Enhanced electromagnetic properties of Fe–Cr–Si alloy powders by sodium silicate treatment. *J. Alloys Compd.* **2015**, *637*, 30–35. [CrossRef]

24. Hsiang, H.I.; Wang, S.K.; Chen, C.C. Electromagnetic properties of FeSiCr alloy powders modified with amorphous SiO_2. *J. Magn. Magn. Mater.* **2020**, *514*, 167151. [CrossRef]

25. Sun, X.; Zhan, J.; Peng, Z. Prepration and characterization of nano-titania surface modified with silica. *J. Chin. Ceram. Soc.* **2007**, *9*, 1174–1177.

26. Wang, J.; Liu, X.; Li, L.; Mao, X. Performance improvement of Fe−6.5Si soft magnetic composites with hybrid phosphate-silica insulation coatings. *J. Cent. South Univ.* **2021**, *28*, 1266–1278. [CrossRef]

27. Liu, D.; Wu, C.; Yan, M. Investigation on sol–gel Al_2O_3 and hybrid phosphate-alumina insulation coatings for FeSiAl soft magnetic composites. *J. Mater. Sci.* **2015**, *50*, 6559–6566. [CrossRef]

28. Li, K.; Cheng, D.; Yu, H.; Liu, Z. Process optimization and magnetic properties of soft magnetic composite cores based on phosphated and mixed resin coated Fe powders. *J. Magn. Magn. Mater.* **2020**, *501*, 166455. [CrossRef]

29. Han, H.; Duan, D.; Yuan, P. Binders and Bonding Mechanism for RHF Briquette Made from Blast Furnace Dust. *ISIJ Int.* **2014**, *54*, 1781–1789. [CrossRef]

30. Luo, Z.; Fan, X.; Hu, W.; Luo, F.; Li, G.; Li, Y.; Liu, X.; Wang, J. Controllable SiO2 insulating layer and magnetic properties for intergranular insulating Fe-6.5wt.%Si/SiO2 composites. *Adv. Powder Technol.* **2019**, *30*, 538–543. [CrossRef]

31. Chang, L.; Xie, L.; Liu, M.; Li, Q.; Dong, Y.; Chang, C.; Wang, X.M.; Inoue, A. Novel Fe-based nanocrystalline powder cores with excellent magnetic properties produced using gas-atomized powder. *J. Magn. Magn. Mater.* **2018**, *452*, 442–456. [CrossRef]

32. Wu, Z.Y.; Jiang, Z.; Fan, X.A.; Zhou, L.J.; Wang, W.L.; Xu, K. Facile synthesis of Fe-6.5wt%Si/SiO2 soft magnetic composites as an efficient soft magnetic composite material at medium and high frequencies. *J. Alloys Compd.* **2018**, *742*, 90–98. [CrossRef]

33. Chang, C.; Guo, J.; Li, Q.; Zhou, S.; Liu, M.; Dong, Y. Improvement of soft magnetic properties of FeSiBPNb amorphous powder cores by addition of FeSi powder. *J. Alloys Compd.* **2019**, *788*, 1177–1181. [CrossRef]

34. Hsiang, H.I.; Fan, L.F.; Hung, J.J. Phosphoric acid addition effect on the microstructure and magnetic properties of iron-based soft magnetic composites. *J. Magn. Magn. Mater.* **2018**, *447*, 1–8. [CrossRef]

35. Li, Z.; Chen, L. Static and dynamic magnetic properties of Co_2Z barium ferrite nanoparticle composites. *J. Mater. Sci.* **2005**, *40*, 719–723. [CrossRef]

36. Shokrollahi, H.; Janghorban, K. Effect of warm compaction on the magnetic and electrical properties of Fe-based soft magnetic composites. *J. Magn. Magn. Mater.* **2007**, *313*, 182–186. [CrossRef]

37. Sugimura, K.; Yabu, N.; Sonehara, M.; Sato, T. Novel Method for Making Surface Insulation Layer on Fe-Based Amorphous Alloy Powder by Surface-Modification Using Two-Step Acid Solution Processing. *IEEE Trans. Magn.* **2018**, *54*, 1–5. [CrossRef]

38. Zhou, B.; Chi, Q.; Dong, Y.; Liu, L.; Zhang, Y.; Chang, L.; Pan, Y.; He, A.; Li, J.; Wang, X. Effects of annealing on the magnetic properties of Fe-based amorphous powder cores with inorganic-organic hybrid insulating layer. *J. Magn. Magn. Mater.* **2020**, *494*, 165827. [CrossRef]

39. Li, T.; Dong, Y.; Liu, L.; Liu, M.; Shi, X.; Dong, X.; Rong, Q. Novel Fe-based nanocrystalline powder cores with high performance prepared by using industrial materials. *Intermetallics* **2018**, *102*, 101–105. [CrossRef]

40. Narayanan, T. Surface pretreatment by phosphate conversion coatings—A review. *Rev. Adv. Mater. Sci.* **2005**, *9*, 130–177.

41. Dong, Y.; Li, Z.; Liu, M.; Chang, C.; Li, F.; Wang, X.M. The effects of field annealing on the magnetic properties of FeSiB amorphous powder cores. *Mater. Res. Bull.* **2017**, *96*, 160–163. [CrossRef]